

Steven L. Morey · Mark A. Bourassa ·  
Dmitry S. Dukhovskoy · James J. O'Brien

## Modeling studies of the upper ocean response to a tropical cyclone

Received: 1 July 2005 / Accepted: 14 April 2006  
© Springer-Verlag 2006

**Abstract** A coupled ocean and boundary layer flux numerical modeling system is used to study the upper ocean response to surface heat and momentum fluxes associated with a major hurricane, namely, Hurricane Dennis (July 2005) in the Gulf of Mexico. A suite of experiments is run using this modeling system, constructed by coupling a Navy Coastal Ocean Model simulation of the Gulf of Mexico to an atmospheric flux model. The modeling system is forced by wind fields produced from satellite scatterometer and atmospheric model wind data, and by numerical weather prediction air temperature data. The experiments are initialized from a data assimilative hindcast model run and then forced by surface fluxes with no assimilation for the time during which Hurricane Dennis impacted the region. Four experiments are run to aid in the analysis: one is forced by heat and momentum fluxes, one by only momentum fluxes, one by only heat fluxes, and one with no surface forcing. An equation describing the change in the upper ocean hurricane heat potential due to the storm is developed. Analysis of the model results show that surface heat fluxes are primarily responsible for widespread reduction ( $0.5^{\circ}$ – $1.5^{\circ}$ C) of sea surface temperature over the inner West Florida Shelf 100–300 km away from the storm center. Momentum fluxes are responsible for stronger surface cooling ( $2^{\circ}$ C) near the center of the storm. The upper ocean heat loss near the storm center of more than  $200 \text{ MJ/m}^2$  is primarily due to the vertical flux of thermal energy between the surface layer and deep ocean. Heat loss to the atmosphere during the storm's passage is approximately  $100$ – $150 \text{ MJ/m}^2$ . The upper ocean cooling is enhanced where the preexisting mixed layer is shallow,

e.g., within a cyclonic circulation feature, although the heat flux to the atmosphere in these locations is markedly reduced.

**Keywords** Air–sea interaction · Tropical cyclones · Ocean modeling · Air–sea fluxes

### 1 Introduction

Understanding the air–sea interaction associated with a tropical cyclone is critical for understanding the development and life cycles of the storms, which can improve storm intensity and track forecasting. It has commonly been accepted that warm sea surface temperatures (SSTs) are favorable for tropical cyclone development by providing the energy necessary for deep atmospheric convection. Much attention has been paid to the cooling of the upper ocean that occurs under a tropical cyclone and how this can modify the heat exchange to the atmosphere during a storm (e.g., Cione and Uhlhorn 2003). Typically, the upper ocean heat content (strongly dependent on mixed layer depth) is of interest in discussions of tropical cyclone forecasting. It has been shown that variations in the mixed layer depth play a significant role in determining the SST response to a tropical cyclone, which in turn causes a feedback to the surface fluxes (Mao et al. 2000). A deeper mixed layer will cool more slowly allowing for prolonged heat loss to the atmosphere. Upwelling and entrainment of cold subsurface water into the mixed layer is the widely accepted mechanism of mixed layer (and SST) cooling under a hurricane (O'Brien 1967a,b; Price 1981). Price (1981) examines the upper ocean response to a hurricane and concludes that entrainment is the primary mechanism for lowering the SST, and that air–sea heat exchange only plays a minor role, although Shen and Ginis (2003) show that the surface heat flux is of primary importance in shallow coastal areas.

Accurate modeling of the ocean response to tropical cyclones has been problematic due to the lack of quality wind fields for forcing. Morey et al. (2005b) presented new techniques for developing wind fields for numerical

---

Responsible editor: Bernard Barnier

---

S. L. Morey (✉) · M. A. Bourassa · D. S. Dukhovskoy ·  
J. J. O'Brien  
Center for Ocean–Atmospheric Prediction Studies,  
The Florida State University,  
Tallahassee, FL 32306-2840, USA  
e-mail: morey@coaps.fsu.edu  
Tel.: +1-850-6440345  
Fax: +1-850-6444841

modeling that compare well with observations during tropical cyclones. These winds combine satellite scatterometer data with numerical weather prediction (NWP) data to produce accurate wind fields uniformly gridded in space and time for numerical ocean models. These wind fields seem to produce a more accurate simulation of the ocean during tropical cyclone forcing than using available NWP winds alone. This paper extends the previous work of Morey et al. (2005b) by applying similar techniques to produce accurate wind fields and investigating the impacts of these wind fields on simulating the ocean's thermodynamic response to a tropical cyclone.

A new coupled ocean and atmospheric boundary layer flux modeling system is developed to examine the upper ocean response to a major hurricane in the Gulf of Mexico, namely, Hurricane Dennis (July 4–13, 2005). The objectively gridded satellite scatterometer wind fields and NWP air temperature data are used to calculate turbulent fluxes across the air–sea interface. Simulations are initialized with a data assimilative “hindcast” of the Gulf to more accurately investigate the impacts of variations in the upper ocean thermal structure on the upper ocean response and air–sea heat fluxes.

Results from a suite of model experiments are analyzed to explain the roles of surface momentum flux (wind stress) and surface heat fluxes on modifying the upper ocean. Surface momentum flux is dominantly responsible for cooling the ocean's surface near the storm's center, and to the right of the storm track, a result consistent with previous works (Price 1981). Model results show that widespread cooling of the sea surface far from the storm track, particularly over the West Florida Shelf (WFS), is largely due to air–sea heat exchange. Examination of the change in Hurricane Heat Potential (HHP) shows that the subsurface response to the storm is largely an effect of the surface momentum flux, with surface heat fluxes playing a secondary role in large-scale cooling of the upper ocean. An equation describing the change in HHP due to the storm is developed. Analysis of the HHP equation verifies that the vertical flux of thermal energy between the upper and deeper layers of the ocean due to upwelling (and subsequent entrainment) is the dominant mechanism by which the upper ocean cools under the storm. This impacts the ocean surface temperature most strongly where the preexisting mixed layer depth is relatively shallow due to a cyclonic circulation feature, as discussed by Walker et al. (2005). The reduction of heat flux to the atmosphere over a cold-core eddy is also documented in the analysis.

---

## 2 Methodology

### 2.1 The numerical simulation

This modeling study is conducted using Navy Coastal Ocean Model (NCOM) numerical simulations of the Gulf of Mexico with an algorithm implemented to compute surface fluxes of heat and momentum. The NCOM was developed at the US Naval Research Laboratory as a

relocatable ocean model originally for use in coupled ocean–atmosphere prediction systems for regional and coastal domains (Martin 2000; Hodur et al. 2002). This model has been applied to geographic domains spanning from the global ocean (Rhodes et al. 2002; Kara et al. 2005) to rather small-scale coastal and estuarine regions (Martin 1999; Morey et al. 2003; Ellingsen 2004).

The NCOM is a primitive equation three-dimensional ocean model with the hydrostatic and Boussinesq approximations and employs a hybrid sigma/z-level vertical coordinate. It supports several numerical differencing and integration methods. For this study, simulations use a quasi-third-order upwind advection scheme (Holland et al. 1998), which reduces the numerical diffusion across fronts and advective overshoots. The Mellor–Yamada Level 2 (Mellor and Yamada 1982) turbulence closure scheme is applied with the Large et al. (1994) background vertical mixing for unresolved processes at near critical Richardson numbers, and consequences of this choice are discussed later. The model is configured for the Gulf of Mexico as described in Morey et al. (2003, 2005a) with 1/20° horizontal resolution and 60 vertical layers (20 evenly spaced sigma or terrain-following grid levels above 100 m, and 40 z-level or geopotential-following grid levels below 100 m to the bottom with stretched grid spacing). This configuration produces a vertical grid spacing of approximately 5 m in the upper 100 m where the ocean depth is greater than 100 m, with closer vertical grid spacing in shallower coastal regions. The model domain encompasses the entire Gulf of Mexico and northwestern Caribbean Sea from 98.15°W to 80.5°W and 15.55° N to 31.5° N, with topography derived from the Smith and Sandwell (1997) data set with manual editing of the coastal areas. The domain has an open boundary to the east with radiation and upwind advection used for outgoing waves and flow, and relaxation to climatology velocity and scalar fields for incoming flow. Freshwater forcing consists of 30 rivers discharging to the Gulf with uniform surface evaporation minus precipitation chosen to balance the annual average river discharge rate.

Four experiments are run for this study: one with momentum fluxes and heat fluxes, one with only momentum fluxes, one with only heat fluxes, and a control case with no surface fluxes. All four experiments are initialized from the model state produced by a “hindcast” run. This hindcast run is forced with surface heat and momentum fluxes described below and assimilates Modular Ocean Data Assimilation System (MODAS; Fox et al. 2002) three-dimensional synthetic temperature and salinity profiles. The NCOM assimilates the MODAS fields using an incremental updating approach where the model scalar fields are incrementally adjusted toward the data at each grid point and time step following an exponential curve with an e-folding scale given by some timescale. The timescale profile was chosen to only weakly assimilate data in the surface mixed layer (with a timescale greater than 7 days), in the deep ocean (greater than 34 days), and over the shelf, and to adjust the subsurface temperature profile most aggressively in the main thermocline (with a time-

scale of about 1 day) where the subsurface temperature variance is largest. This approach serves the purpose of adjusting the ocean model's mesoscale features (eddies and the loop current), and, thus, velocity field toward observations while letting surface fluxes and freshwater point sources dominantly control the mixed layer temperature and salinity distributions.

## 2.2 Heat and momentum fluxes

An atmospheric flux model based on the Bourassa–Vincent–Wood (BVW) boundary layer model (Bourassa et al. 1999) is coupled to the NCOM. The BVW flux model, based on momentum, heat, and moisture roughness length parameterizations, calculates air–sea fluxes of momentum, latent heat, and sensible heat dependent on the air–sea surface temperature and humidity differences, as well as the sea state and the influence of capillary waves. For the experiments presented here, the flux model is simplified by assuming local wind–wave equilibrium, a prescribed surface air humidity of 98%, and a 2-m specific humidity of 20 g/kg. Calculations of the surface momentum, sensible heat, and latent heat fluxes then reduce to functions of the air–sea temperature difference and the 10-m wind velocity for these experiments. Data collected from NOAA National Data Buoy Center station 42039 (29.79°N 86.02°W) show the specific humidity ranging from roughly 18.0 to 20.5 g/kg on July 10, 2005, the day that Hurricane Dennis passed by. Approximation of the specific humidity by a constant 20 g/kg results in an upper bound on the error in the latent heat flux of 18% for 20 m/s wind speed and a 2°C air–sea temperature difference. These simplifications in the flux computations reduce the number of exogenous variables needed to run the comparative model experiments.

The BVW model is used to calculate the friction velocity  $\mathbf{u}_*$ , and analogous scalar quantities  $\theta_*$  (a characteristic temperature) and  $q_*$  (a characteristic humidity). The surface downward momentum flux  $\boldsymbol{\tau}$  and upward latent and sensible heat fluxes  $Q_{\text{sens}}$  and  $Q_{\text{lat}}$  are then calculated as

$$\boldsymbol{\tau} = \rho_A \mathbf{u}_* |\mathbf{u}_*| \quad (1)$$

$$Q_{\text{sens}} = \rho_A C_p \theta_* |\mathbf{u}_*| \quad (2)$$

$$Q_{\text{lat}} = \rho_A L_v q_* |\mathbf{u}_*| \quad (3)$$

where  $\rho_A$  is the air density,  $C_p$  is the specific heat of air, and  $L_v$  is the latent heat of evaporation. This approach bypasses the need to estimate transfer coefficients for calculating the fluxes. The flux model instead uses a sophisticated physically based calculation of roughness lengths (for momentum, heat, and moisture) to convert between input variables and the  $\mathbf{u}_*$ ,  $q_*$ , and  $\theta_*$  (Bourassa et al. 1999; Bourassa 2004).

Air temperatures for these experiments are obtained from the global 1.9° resolution NCEP-DOE AMIP-II Reanalysis (National Center for Environmental Prediction—Department of Energy Atmospheric Model Intercomparison Project Reanalysis 2—hereafter NCEPR2). Solar radiation is prescribed using the DaSilva et al. (1994) monthly climatology for net longwave and shortwave radiation with a Jerlov type III attenuation profile in the ocean model.

To produce the wind fields, 10-m winds are derived from backscatter data from the SeaWinds scatterometer aboard the polar orbiting QuikSCAT satellite. The scatterometer wind data are objectively mapped to a 12° grid every 12 h using the NCEPR2 atmospheric model winds as a background field, as in Morey et al. (2005b). Although the scatterometer winds are equivalent neutral winds (Verschell et al. 1999) mapped to a uniform grid, they are treated as winds for this application, an assumption that gives rise to very small errors (less than 0.5 m/s). This approach allows a feedback from the modeled SST to the surface momentum and heat fluxes via atmospheric stability. That is, the friction velocity, which is used to calculate momentum and heat fluxes, becomes a function of stability. Morey et al. (2005b) analyze this wind product by forcing a nondata assimilative Gulf of Mexico ocean model with the winds from mid-1999 through the end of 2000 and comparing the model results over the WFS with in situ observations. The wind fields are also compared to observed winds at several locations throughout the Gulf. The wind product is found to perform well compared to atmospheric model data and has increased accuracy for energetic events such as tropical cyclones.

The input fields to the flux model consist of the air temperature and gridded 10-m wind fields, linearly interpolated to the ocean model horizontal grid and time step, along with the ocean model sea surface temperature (SST); these input fields are used to calculate the surface fluxes at every ocean model surface grid point and time step. The model is run with the surface fluxes and data assimilation for June 21–July 8, 2005, to initialize the Hurricane Dennis model experiments, which are run from July 8 to July 12, 2005.

## 2.3 Model experiments

Four numerical model experiments are conducted to study the case of Hurricane Dennis. This storm was tracked by the National Hurricane Center (NHC) from July 4 to July 13, 2005, making its final landfall in the western Florida panhandle at 1930 UTC on July 10 (Figs. 1 and 2). Dennis began as a tropical depression in the Caribbean over the southern Windward Islands and made landfall as a category 4 hurricane in southeastern Cuba on July 8. The storm passed over Cuba and into the Gulf of Mexico after weakening to a category 1 storm. Dennis intensified and traveled north–northwestward just offshore of the WFS with maximum sustained winds peaking at 64 m/s at 1200

UTC on July 10 with a central pressure of 930 mbar, weakening before striking Florida. The storm translation speed was generally around 6 m/s. In the Gulf, hurricane force winds were confined to a small area near the eye, but tropical storm force winds extended far (about 350 km) from the center over southern Florida and the Florida panhandle (Beven 2005). These characteristics present the opportunity for analysis of the modeled air–sea fluxes and ocean response near the center of the strong storm and over a broad shelf under tropical storm force winds.

Each of the four model experiments is initialized at 00 UTC on July 8, 2005, from the output of the data assimilative hindcast run. The initial SST field compares well with the TMI (TRMM Microwave Radiometer) satellite 3-day composite SST, except for in the southwestern Gulf where the model shows pronounced upwelling typical of this time of year (Zavala-Hidalgo et al. 2006) and in the Caribbean (likely due to the application of climatology temperature fields at the open boundary; see Fig. 2). It should be noted that the central Gulf is generally cooler than the rest of the basin, by 0.5–1°C. This is due to the passage of Hurricane Cindy on July 3–7, 2005, just before Hurricane Dennis. It is likely that there is an impact of this cooling produced by Cindy on the heat fluxes during Hurricane Dennis.

After initialization of the experiments, they are run with no data assimilation for 4 days. These experiments are identical to each other, except for the manner in which surface fluxes are applied. For the first experiment, the BVW flux model is used to calculate surface momentum and heat fluxes (the MFHF experiment). The second experiment is run with only momentum fluxes (MF experiment) and an insulated surface. No heat flux is permitted through the surface (including radiation), although the air–sea temperature difference is still used to calculate the wind stress. In the third experiment, only heat fluxes are applied (HF experiment), although the wind data are still used to calculate the heat fluxes. The last experiment has no surface fluxes (NF experiment) and is used to compute the HHP and SST anomalies for analyzing the other experiments.

## 3 Results

### 3.1 Surface momentum and heat fluxes

The modeled net latent and sensible heat flux from the ocean is greater than 400 W/m<sup>2</sup> (positive from the ocean to atmosphere) throughout a large area of the eastern Gulf of Mexico during the storm (Fig. 1). The largest heat fluxes are more than 900 W/m<sup>2</sup> to a maximum of 1,115 W/m<sup>2</sup> northeast of the storm center, where the strongest winds are found in the gridded wind fields. These values can be compared to the inner core heat flux estimates of 650–2,600 W/m<sup>2</sup> used by Cione and Uhlhorn (2003) in their analysis of SST variability in hurricanes. In their analysis, they reported an average inner core total surface enthalpy flux of approximately 1,300 W/m<sup>2</sup> for a category 1 storm

(wind speeds of 33–43 m/s<sup>2</sup>). The 1/2° resolution wind fields used for these experiments do not resolve the inner core structure, but provide good accuracy for the wind field outside the storm's intense core (Morey et al. 2005b). Thus, the heat fluxes are likely underestimated directly around the storm center, on the scale of a few radii of maximum winds. An analysis of the wind stress curl time series at 26° N 85.3°W (a location of more detailed analysis below) computed from the gridded wind fields yields a maximum of  $1.5 \times 10^{-4}$  N/m<sup>3</sup> (for reference, the NHC track shows Dennis centered at 26.1°N 85.0°W at 00UTC on July 10).

### 3.2 Sea surface temperature response

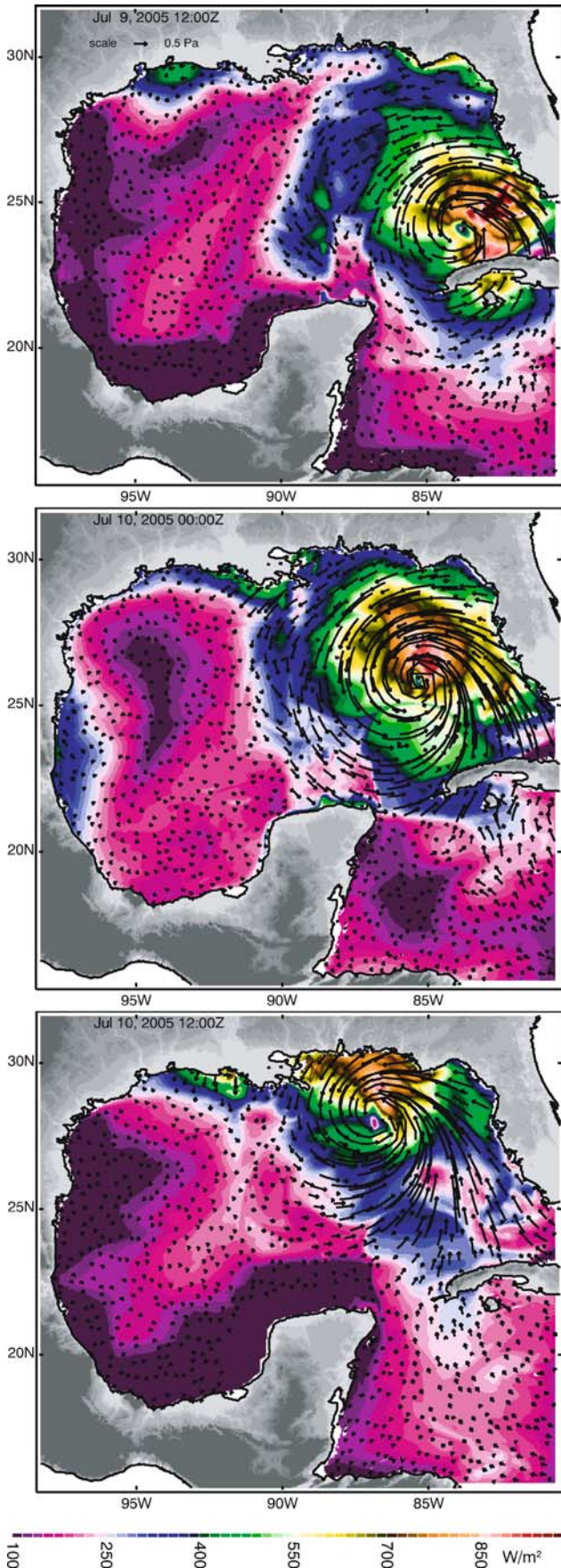
The change in SST due to Hurricane Dennis is approximated by the SST anomaly obtained by subtracting the NF SST field from the SST fields of the other experiments. This is done to reduce the impacts of migrating fronts and eddies on the analysis of the SST response. The movements of these deep mesoscale features are largely insensitive to surface forcing at these timescales. Inspection of these SST anomalies shows that the MFHF experiment produces pronounced cooling of the sea surface over the eastern Gulf of Mexico during the passage of Hurricane Dennis (Fig. 2). The coastal regions are cooled rapidly due to the surface heat loss being distributed over shallow water depths. Away from the coast, the strongest cooling associated with the storm is evident just offshore of the WFS where the temperature change is nearly 2°C. Three-day composite SST images from TMI satellite data show a similar cooling pattern in the eastern Gulf (Fig. 2), but stronger by about 1°C.

Away from the inner continental shelf, the MF experiment produced SST anomalies similar to the MFHF experiment, highlighting the importance of momentum fluxes on governing the SST response. The HF experiment does not show the extreme cooling near the storm center, but does produce cooling over the WFS of 0.5–1.0°C, with more pronounced cooling in the shallow water near the coast. The rapid cooling of shallow coastal waters due to surface heat loss during a tropical cyclone is discussed by Shen and Ginis (2003).

### 3.3 Subsurface thermal response

In satellite SST observations and numerical model results, a region of strong surface cooling is found near 26–26.5°N 85°W, offshore of the continental shelf break (Fig. 2).

Inspection of a synoptic map of the model depth of the 26° isotherm (below the mixed layer) shows that the region of strongest cooling offshore of the WFS is also the location of a cyclonic eddy at the eastern edge of the constriction between a recently detached anticyclonic Loop Current Eddy and the Loop Current (Fig. 3). In this cold-core eddy, the 26°C isotherm is lifted to within 35 m of the surface, compared to its mean depth of 57 m in the Gulf of Mexico.



◀ **Fig. 1** Surface heat fluxes (latent plus sensible,  $\text{W/m}^2$  positive upward) calculated from the model with wind stress vectors overlain. The three panels are synoptic maps at 12-h intervals

A time series of the temperature profile within this eddy illustrates the transformation that the subsurface thermal structure undergoes during the storm (Fig. 4). Rapid upwelling due to the Ekman divergence caused by the cyclonic winds (positive wind stress curl) is clearly evident at the time the storm passes overhead on July 10. The subsurface isotherms are raised more than 15 m in about 12 h. The mixed layer depth initially deepens from 16 to 24 m before the storm, and then shallows rapidly to 8 m. The temperature within the mixed layer at this location decreases by  $2^\circ\text{C}$  before slightly warming after the storm passage. Oscillations of the isotherms at a near-inertial period (the inertial period is 26.8 h at this location) can also be seen following the storm. Upwelling and near-inertial internal gravity waves are consistent with earlier work on the impacts of moving storms on the upper ocean (Shay et al. 1992; Mao et al. 2000; Zedler et al. 2002).

In the MF experiment, a similar subsurface thermal response is evident. Cooling of the mixed layer during July 10 is not as rapid; however, the mixed layer does not begin to warm after the storm because there is no stabilizing heat flux (solar radiation). Thus, the mixed layer (and surface) temperature at the end of the experiment is actually slightly cooler than the MFHF case.

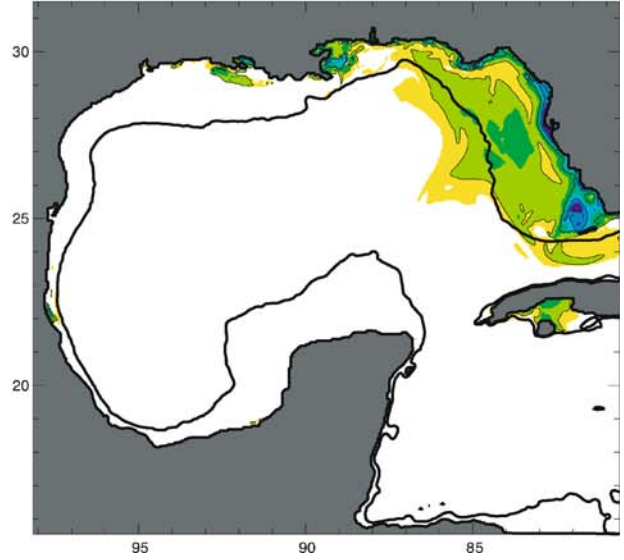
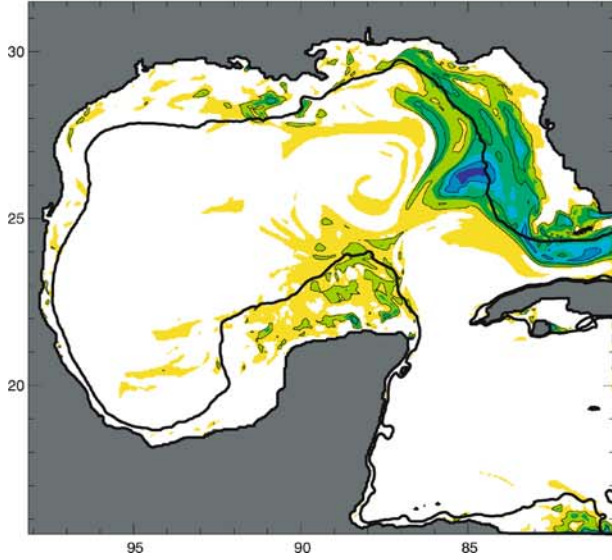
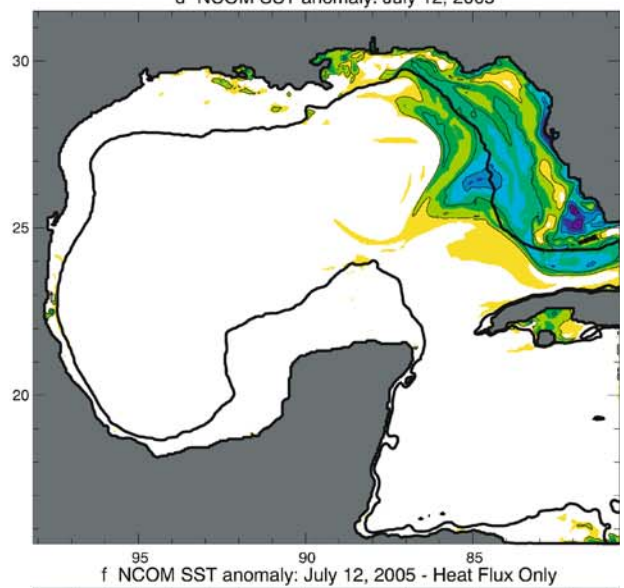
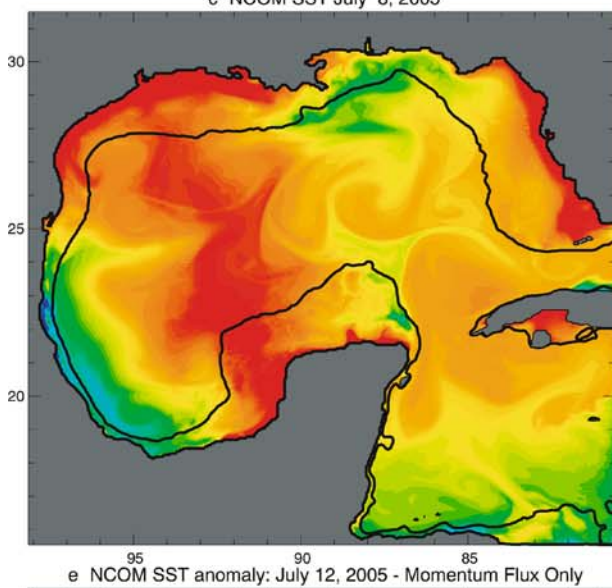
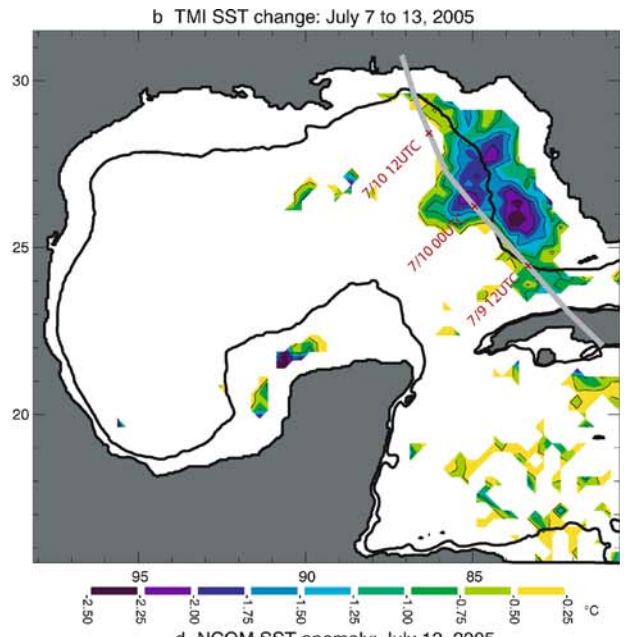
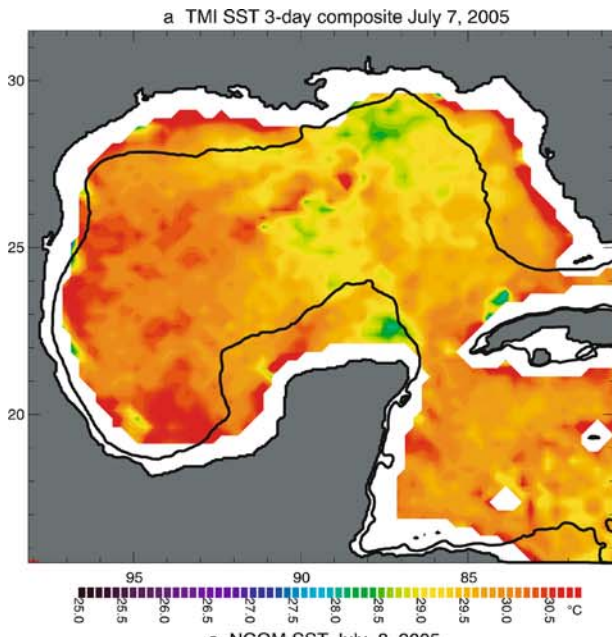
For the HF experiment, the temperature profile time series shows no upwelling, nor amplification of waves at near-inertial periods due to the storm. This result is expected since there is no momentum flux to generate upwelling or a significant dynamical response. The mixed layer is uniformly cooled by just less than  $1^\circ\text{C}$  and deepens by 3–5 m throughout the experiment.

### 3.4 Heat budget analysis

Leipper and Volgenau (1972) introduce the quantity Hurricane Heat Potential (HHP), which is approximately the ocean's thermal energy available to a tropical cyclone. In continuous form, it can be calculated as

$$HHP = \int_{-D_{T_{ref}}}^{\eta} \rho c_p (T(z) - T_{ref}) dz \quad (4)$$

where  $\eta$  is the height of the ocean surface above its resting geopotential surface,  $T$  is the potential temperature,  $c_p$  is the specific heat of seawater,  $\rho$  is the water density, and  $D_{T_{ref}}$  is the depth of the reference temperature  $T_{ref}$ . Typically,  $T_{ref}=26^\circ\text{C}$ , which is considered to be the water temperature below which a hurricane does not form. This quantity can be viewed as the ocean heat energy available to be extracted by a hurricane, or as the ocean heat content above the  $26^\circ\text{C}$  isotherm relative to a  $26^\circ\text{C}$  mixed layer of the same depth.



◀ **Fig. 2** **a** TMI 3-day composite SST centered on July 7, 2005. **b** SST change from the TMI 3-day composite SST centered on July 7 to July 13, 2005. **c** Model SST synoptic map from July 8, 2005. **d** Model SST anomaly (from the NF experiment) for the MFHF experiment on July 12, 2005. **e** SST anomaly for the MF experiment. **f** SST anomaly for the HF experiment. *White areas* denote either SST changes greater than  $-0.25^\circ$  or lack of data near the coastal areas for the TMI images. Note all dates correspond to 00UTC. A schematic of the track of Hurricane Dennis is overlaid in **b**, estimated from the official NHC track. The 200-m isobath is drawn in this and subsequent figures

The HHP spatial pattern follows closely the  $26^\circ\text{C}$  isotherm depth (Fig. 5). The Loop Current and anticyclonic Loop Current Eddy appear as large heat reservoirs, and the cyclone centered near  $26^\circ\text{N}$   $85^\circ\text{W}$  appears as a local minimum. Although it seems intuitive to calculate the difference in HHP before and after the storm, it turns out that displacements of deep mesoscale features due to dynamics unrelated to the surface forcing can cause large spatial variability in the HHP difference that hinders analysis of the storm's impact. Therefore, the HHP anomaly is calculated in a similar fashion to the SST anomaly. The HHP from the NF experiment is subtracted from the HHP field of each of the other experiments to produce the change in HHP due to the storm (Fig. 5).

The HHP anomaly from the MFHF experiment generally shows a loss of heat above the  $26^\circ$  isotherm in the eastern Gulf waters that were impacted by Hurricane Dennis, with slight warming to the west. The strongest HHP anomalies of  $-100$  to  $-150$   $\text{MJ}/\text{m}^2$  occur very close to the storm track, with an area of large anomalies collocated with the cyclonic eddy. The MF experiment produces cold anomalies in a similar pattern,

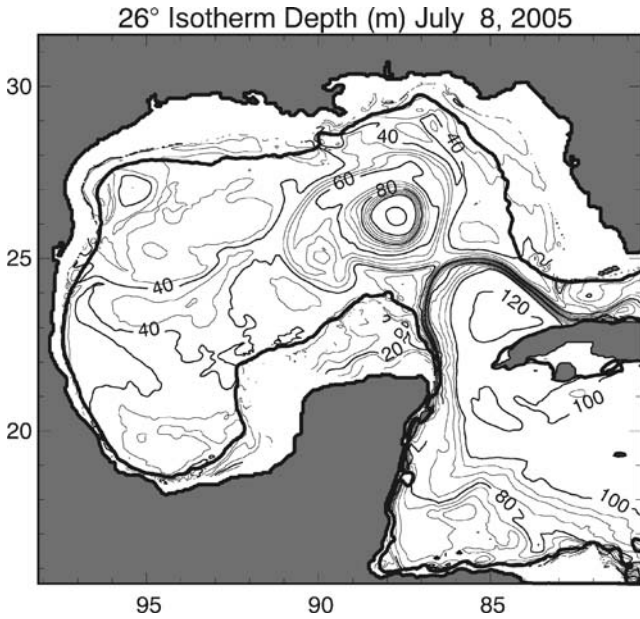


**Fig. 3** Depth of the model  $26^\circ\text{C}$  isotherm on July 8, 2005, the initialization time for the four Hurricane Dennis experiments. The contour interval is 5 m from 0 to 100 m and 20 m for depths greater than 100 m. *Thick contours* are drawn every 20 m, and contours are not drawn where the entire water column is warmer than  $26^\circ$  on the shelf

but without the heating of the western Gulf due to the lack of solar radiation. The HHP anomalies from the HF experiment have much less spatial variability. The anomalies are in the range of 0 to  $-50$   $\text{MJ}/\text{m}^2$ . From the SST anomalies (Fig. 2), it is likely that there is substantial heat energy loss over the shallow inner shelf, but the HHP is not defined in these areas where the entire water column exceeds  $26^\circ\text{C}$ .

An equation describing the rate of change of HHP anomaly can be derived and integrated in time through the model experiments to aid in analyzing the upper ocean response to the hurricane. The NCOM temperature equation in continuous form is

$$\frac{\partial T}{\partial t} = -\nabla \cdot (\mathbf{v}T) + \frac{\partial}{\partial z} \left( K_H \frac{\partial T}{\partial z} \right) + \frac{Q_{\text{rad}}}{\rho c_p} \frac{\partial \gamma}{\partial z} \quad (5)$$

where

$$\nabla \cdot \mathbf{v} = \frac{\partial u}{\partial x} + \frac{\partial v}{\partial y} + \frac{\partial w}{\partial z} = 0 \quad (6)$$

$$K_H \frac{\partial T}{\partial z} = \frac{Q_{\text{net}}}{\rho c_p} \text{ at } z = \eta. \quad (7)$$

$u$ ,  $v$ , and  $w$  are the eastward, northward, and upward velocity components in the  $x$ ,  $y$ , and  $z$  directions, respectively. In Eq. (5), the source term (rivers, for example) is excluded, and the horizontal diffusion term is not included because the quasi-third-order upwind advection scheme of Holland et al. (1998) used in the experiments includes a biharmonic mixing term.  $K_H$  is the vertical eddy coefficient for scalar fields,  $Q_{\text{rad}}$  is the net downward solar radiation ( $\text{W}/\text{m}^2$ ),  $\gamma$  is a function describing the extinction of solar radiation with depth, and  $Q_{\text{net}}$  is the net downward surface (latent plus sensible) heat flux ( $\text{W}/\text{m}^2$ ). If a rigid lid ( $\eta=0$ ) is assumed and  $\rho$  and  $c_p$  are taken as constants, then vertical integration of Eq. 5 from  $z=-D(t)$  to  $z=0$  [where  $D(t)$  is the depth of the  $26^\circ\text{C}$  isotherm] results in the hurricane heat potential equation

$$\begin{aligned} \frac{\partial \text{HPP}}{\partial t} = & -\rho c_p \int_{-D(t)}^0 \left( u \frac{\partial T}{\partial x} + v \frac{\partial T}{\partial y} \right) dz \\ & -\rho c_p \int_{-D(t)}^0 w \frac{\partial T}{\partial z} dz - \rho c_p K_H \frac{\partial T}{\partial z} \Big|_{z=-D(t)} \\ & + Q_{\text{net}} + Q_{\text{rad}} \end{aligned} \quad (8)$$

The left hand side of Eq. (8) is the time rate of change of HPP, and the terms on the right hand side represent in order the time rate of change of HPP due to horizontal temperature advection, vertical temperature advection, vertical mixing across the lower boundary, net downward surface heat flux, and net downward solar radiation, which was simplified by

approximating  $\gamma(-D) \approx 0$ . Equation (8) resembles the heat budget equation for an upper mixed layer, except that there can be variations in the temperature profile down to 26°C. Because no instantaneous mixing is assumed to occur when colder water outcrops through the lower boundary (where the water column is typically still stratified), an obvious entrainment term does not appear. However, the vertical temperature advection term can be rewritten as

$$\begin{aligned} \rho c_p \int_{-D(t)}^0 w \frac{\partial T}{\partial z} dz &= \rho c_p \int_{-D(t)}^0 \left( \frac{\partial w T}{\partial z} - T \frac{\partial w}{\partial z} \right) dz \\ &\approx \rho c_p \int_{-D(t)}^0 \left( \frac{\partial w T}{\partial z} - \bar{T} \frac{\partial w}{\partial z} \right) dz \end{aligned} \quad (9)$$

where  $\bar{T}$  is the depth-averaged temperature above the  $T_{ref}=26^\circ\text{C}$  isotherm. The last integral of Eq. (9) then simplifies to

$$\rho c_p \int_{-D(t)}^0 \left( \frac{\partial w T}{\partial z} - \bar{T} \frac{\partial w}{\partial z} \right) dz = \rho c_p (\bar{T} - T_{ref}) w(-D(t)). \quad (10)$$

This term now appears as a vertical thermal energy flux (VTEF) across the 26°C isotherm and stands in place of the typical upwelling and entrainment terms.

Subtracting the terms in Eq. (8) computed from the NF experiment from the terms computed from the MFHF experiment results in a balance for the HHP anomaly. When this equation is integrated in time, it describes the processes responsible for the change in the HHP anomaly during the integration period. The vertical mixing term is not computed because stratification at the 26°C isotherm causes  $K_H$  to be small and the term is unimportant (as will become evident when the balance of terms is discussed later). This would not necessarily be the case if a reference temperature were chosen with an isotherm depth closer to the mixed layer depth.

The time integral from July 8 00UTC to July 12 00UTC of the terms of the HHP anomaly equation are computed for the MFHF experiment (Fig. 6) and can be compared to the HHP anomaly map for the same experiment (Fig. 5b). Inspection of the fields shows that the VTEF term (which is due to upwelling) dominates the change in HHP during the hurricane in deep water. The horizontal advection term does not show a clear warming or cooling pattern along the storm track. Computing the anomaly from the NF experiment reduces the impact of the strong circulation features on the HHP change, but small differences in the locations of the features between experiments still result in locally large impacts on the upper ocean heat content, which reflects on the HHP, near the Loop Current and eddies.

The combined net surface (sensible plus latent) heat flux and radiation terms contribute  $-30$  to  $-50$  MJ/m<sup>2</sup> to the HHP budget (a heat energy loss) under the storm similar to the net heat loss in the HF experiment (Fig. 5d). Since the solar radiation in this experiment contributes between 70

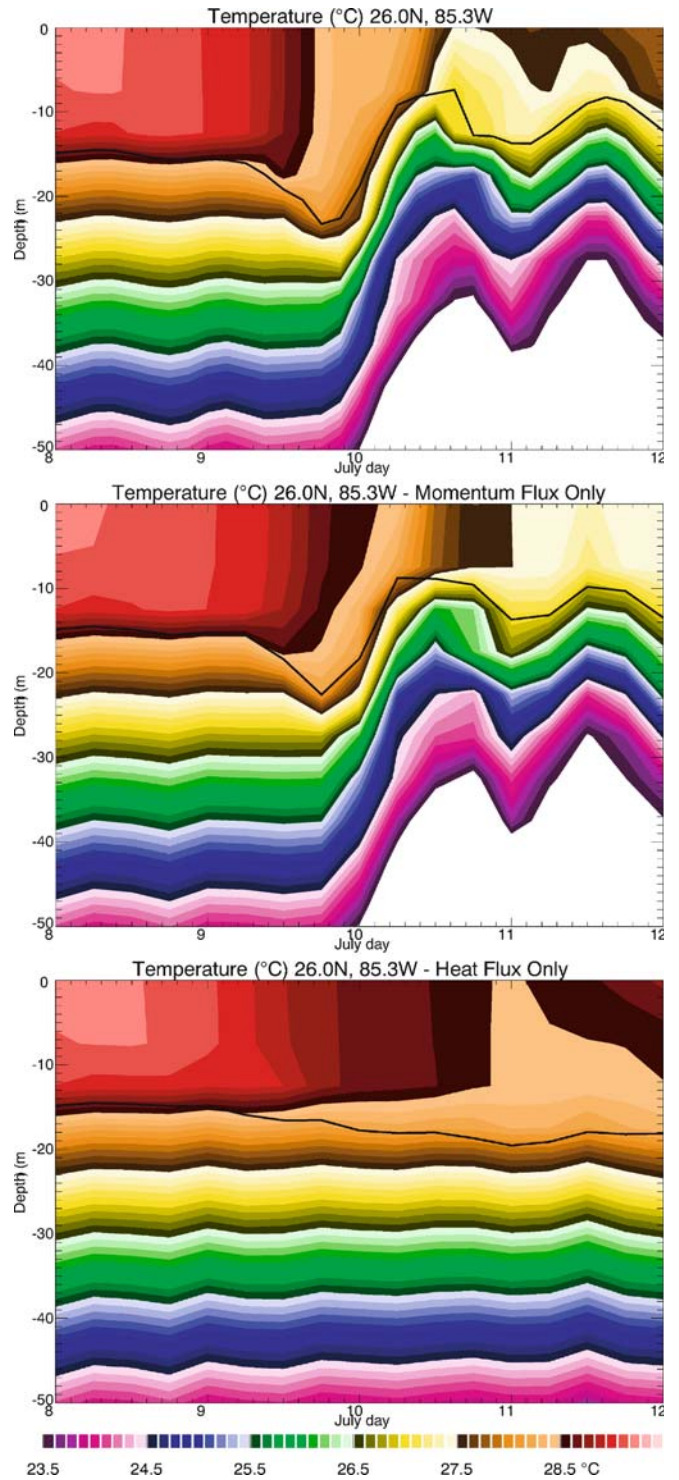


**Fig. 4** Time series of the temperature profile at 26°N, 85.3°W for the MFHF experiment (*top*), the MF experiment (*middle*), and the HF experiment (*bottom*). The mixed layer depth estimated using  $T_{surface}-0.5\text{C}$  is shown with a *black line* on each panel. *White areas* denote water colder than 23.5°C

and 100 MJ/m<sup>2</sup> of heat energy to the ocean, this implies that the heat extracted from the ocean by the atmosphere is between 100 and 150 MJ/m<sup>2</sup>. The model HHP values near the storm track before the hurricane range from about 300 to

1,000 MJ/m<sup>2</sup>. This implies that an estimated 10 to 50% of the heat energy available to the storm is extracted by the atmosphere during the storm's passage. These values are significantly larger than the Cione and Uhlhorn (2003) estimates, which are 2 to 8% utilization of the available heat energy during the passage of the storm core (120 km diameter) under various scenarios. A map of the heat energy extracted by the atmosphere (sensible plus latent heat flux) as a percentage of initial HHP (Fig. 6) shows that the most efficient heat energy utilization occurs where the initial HHP is smallest due to a shallow thermocline. This larger estimate of heat energy utilization could be attributed to the fact that it is being calculated over the entire storm wind field over several days instead of just within the storm core.

Along the storm track, a local minimum in the surface heat loss magnitude can be found near the cyclonic eddy at

26°N 85.3°W. This is the result of the negative feedback from the surface temperature on the surface heat loss. The presence of cold water near the surface leads to rapid cooling due to vertical thermal energy flux between the surface waters and deeper layers, resulting in a reduced surface temperature and reduced heat loss to the atmosphere.

Near the center of the above-mentioned cyclonic eddy, where strong cooling was observed with a large reduction in HHP in the model experiments, the balance of terms for the time integrated HHP anomaly equation is examined (Fig. 7). Here, not far from the storm center, the VTEF term plays a dominant role in reducing the heat content above the 26°C isotherm. Horizontal temperature advection caused by the storm winds does not contribute significantly (away from the eddy edge and its strong circulation, small differences in eddy position between the MFHF and NF

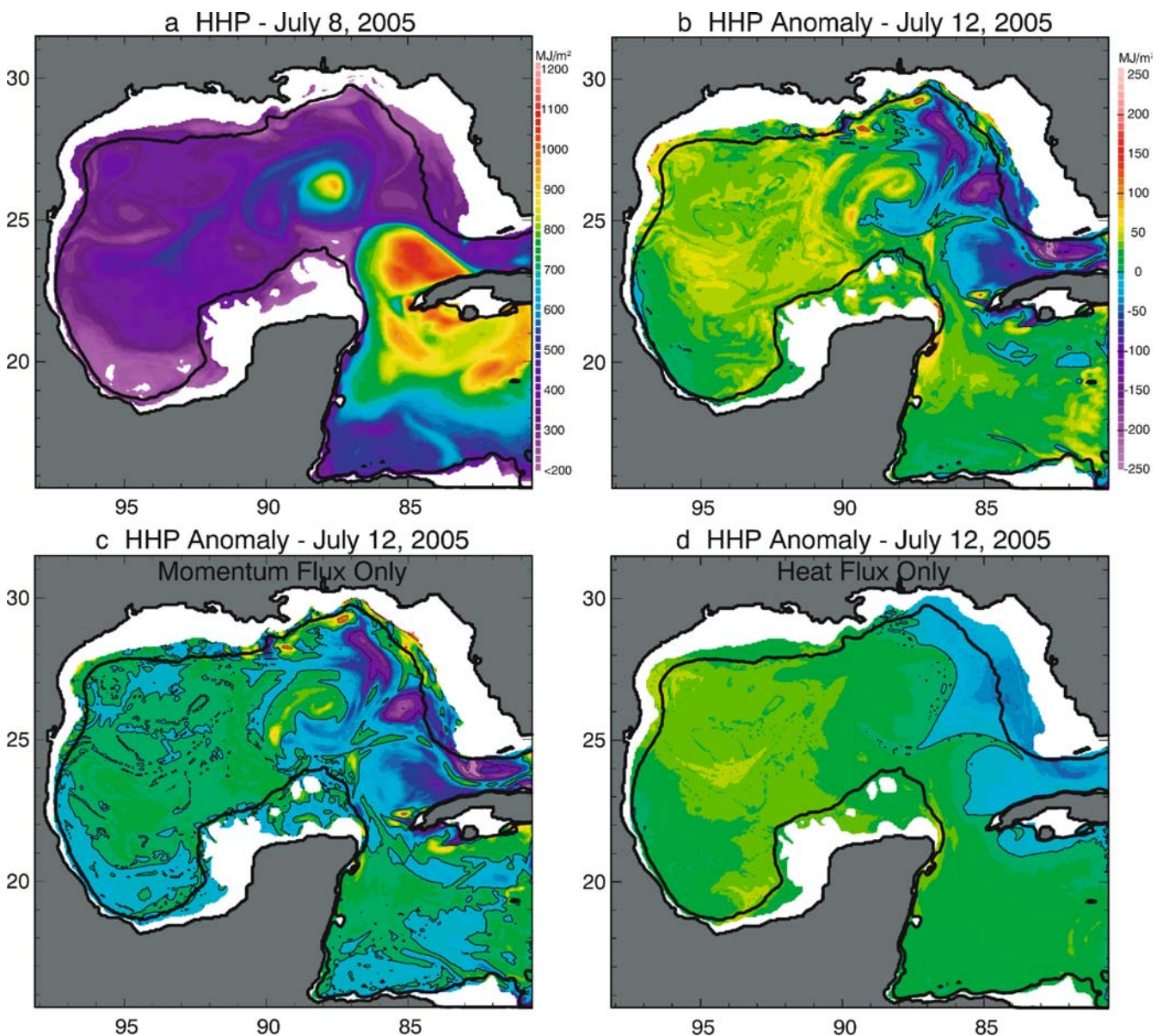


**Fig. 5** a Model Hurricane Heat Potential (HHP) on July 8, 2005. b–d HHP anomaly (from the NF experiment) on July 12, 2005 for the MFHF experiment (b), the MF experiment (c), and the HF experiment (d)

experiments do not confuse the analysis of this term as is seen elsewhere in the domain in Fig. 6). The heat loss to the atmosphere is nearly  $100 \text{ MJ/m}^2$  and compensates the solar radiation input and the small horizontal advection term. Summing the VTEF, horizontal advection, surface heat flux, and solar radiation terms verifies that these terms result in a good balance even when the vertical mixing term is neglected. Furthermore, the small horizontal advection term suggests that a one-dimensional balance would apply reasonably well, although it should be noted that horizontal divergence is necessary to achieve the vertical velocity important for the vertical thermal energy flux.

#### 4 Discussion

The set of numerical experiments described in this paper is intended to provide insight into the surface heat and momentum fluxes during a tropical cyclone and their roles in modifying the upper ocean. Understanding how to better simulate the upper ocean thermal response model to the passage of a tropical cyclone is critical to predicting the life cycle of the storm. The modeling system presented in this paper is a step toward improving the calculation of fluxes in a physically based manner using a sophisticated ocean model and new techniques of creating wind fields, although the resolution of the wind fields is still too coarse

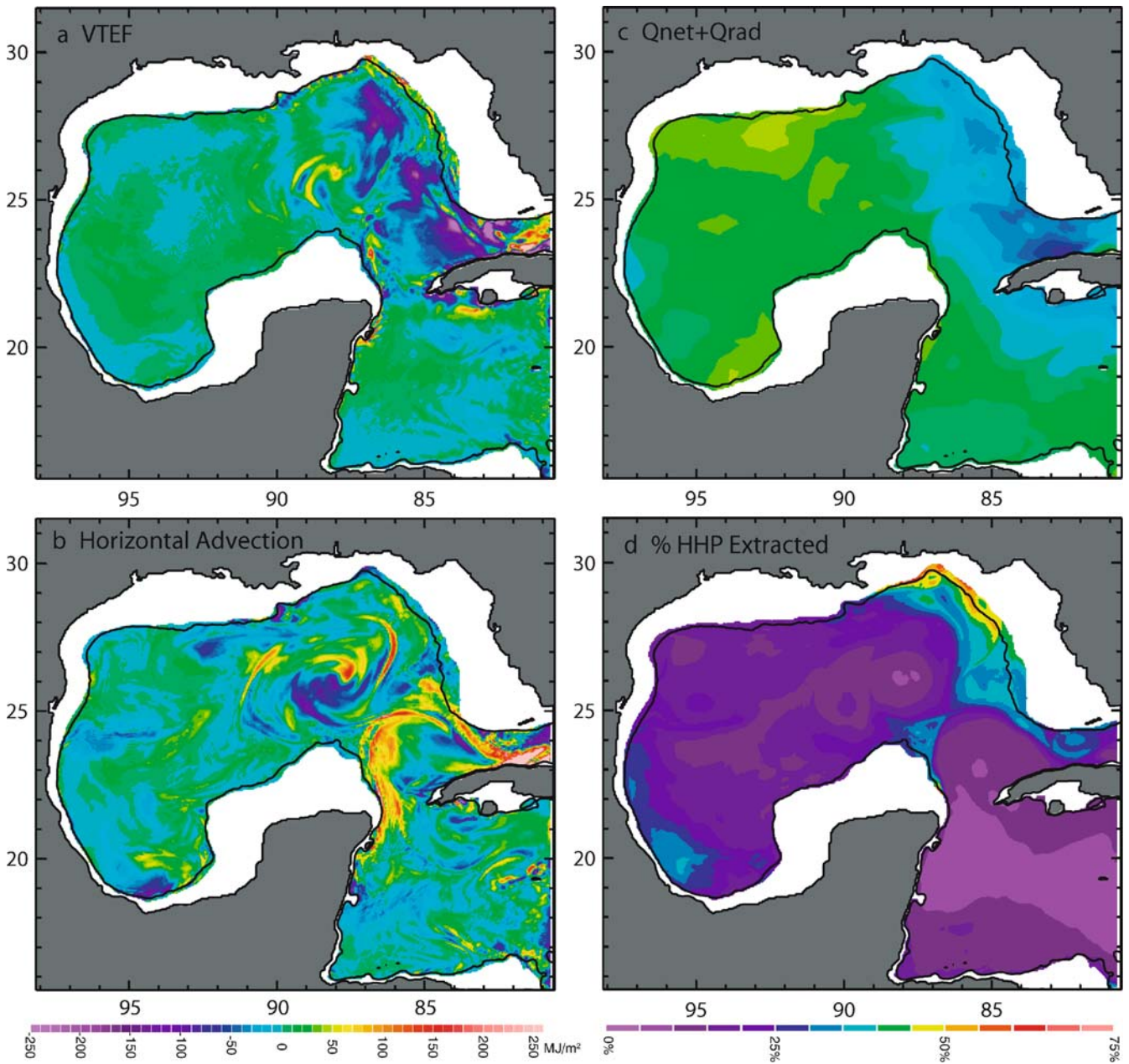
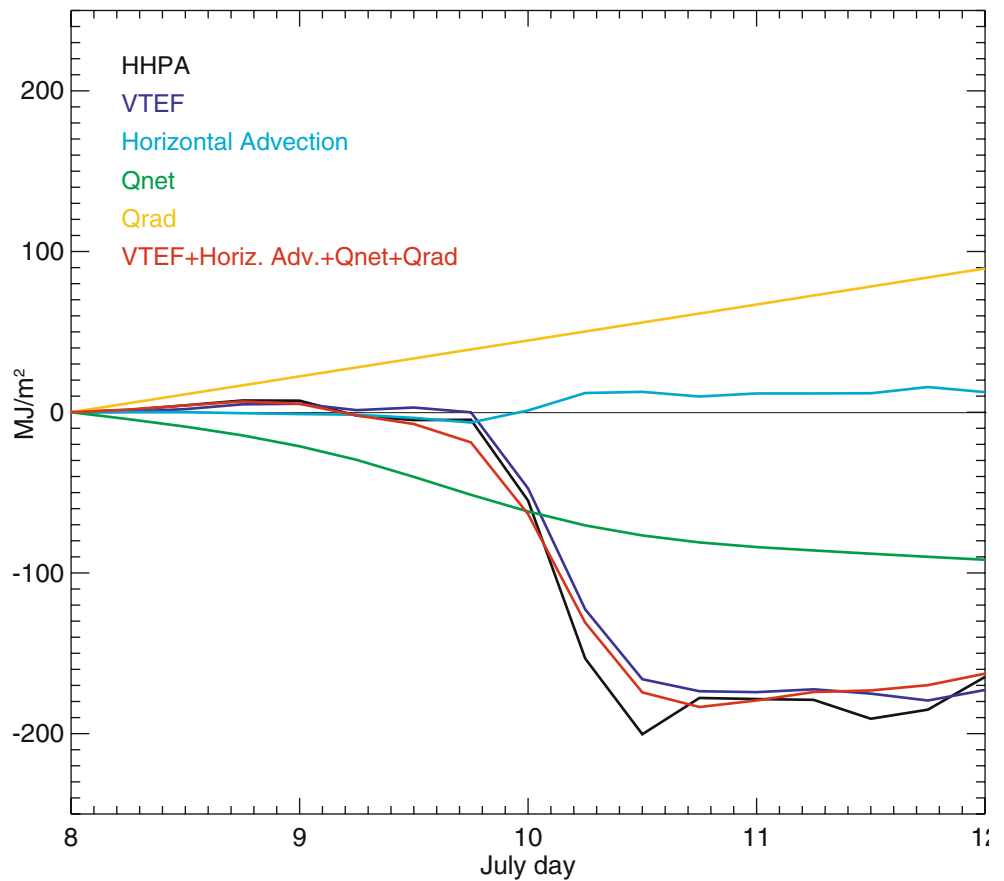


**Fig. 6** a–c Maps of the terms of the HHPA equation integrated in time from July 8 00UTC to July 12 00UTC. **d** Heat energy extracted by the atmosphere (sensible plus latent heat flux) as a percentage of

initial HHP during the model integration. The *left color bar* ( $\text{MJ/m}^2$ ) applies to a–c, and the *right color bar* (%) applies to **d**

**Fig. 7** Terms of the HHPA equation integrated in time from July 8 00UTC to the time shown on the abscissa. The sum of the terms (except the horizontal and vertical mixing terms) is shown by the red line



to accurately simulate the processes near a storm's central core. A number of simplifications were made to the complicated flux model to reduce the variables for model experiment intercomparisons. It is anticipated that the modeling system can be further developed by relaxing the simplifications and assumptions (such as climatology solar radiation, constant surface freshwater flux, local wind-wave equilibrium, constant specific humidity, etc.) to achieve more accurate calculations of the surface fluxes and simulations of the ocean during tropical cyclones.

The ocean model is configured to produce a realistic response to the surface turbulent fluxes so the ocean feedback to the fluxes can be examined. The ocean model has very high horizontal and vertical resolutions, and is initialized using a data assimilative hindcast to accurately represent the state of the ocean during the hurricane. An important consideration, though, is the manner in which the vertical mixing is computed, which is critical to achieving an accurate mixed layer depth. The experiments presented in this paper use the Mellor and Yamada Level 2 (MYL2) turbulence closure scheme, with the addition of a background vertical mixing value near critical Richardson numbers to account for unresolved processes (Large et al. 1994), to calculate the vertical eddy coefficients for momentum and scalar fields. Local vertical shear provides the source for TKE (turbulent kinetic energy) in a stably stratified water column using MYL2. However, the addition of a diffusion term to the TKE equation in the MYL2 12 model (Mellor and Yamada 1982) was shown to only

marginally increase the mixed layer depths (Martin 1985). Zedler et al. (2002) show that these turbulence models lead to less surface cooling than the K profile parameterization model, which produces cooling at the surface and throughout the upper water column that more closely matches observations. This, along with the lack of very strong winds in the gridded wind fields near the storm core, could partly explain why the model experiments underpredict the surface cooling seen in the satellite observations.

Although experiments were conducted treating heat fluxes and momentum fluxes separately, it should not be expected that their impacts can be linearly separated. On the contrary, feedback from the ocean surface temperature to the atmosphere affects the magnitude of the fluxes, as can be seen by the reduced heat loss to the atmosphere where strong cooling by upwelling occurs at the center of a cyclonic eddy. It is also important to note that, although the same air temperature and 10-m wind data were used to calculate fluxes for all experiments, the fluxes are not identical for each experiment due to their dependence on the model SST.

## 5 Conclusions

Four numerical experiments conducted with a coupled ocean and atmospheric flux modeling system are used to explore the roles of heat and momentum fluxes in modifying the upper ocean thermal structure during a

hurricane. In addition, the implementation of the Bourassa et al. (1999) flux model, with simplifying assumptions using advanced satellite scatterometer derived wind fields, provides a useful tool for hurricane research and for computing the surface turbulent fluxes associated with the storms.

The model experiments show that the vertical thermal energy flux due to upwelling is dominantly responsible for cooling the upper ocean near the storm center. Over the shallow continental shelf, this process cannot occur, and surface heat loss to the atmosphere dominates the ocean cooling. In the case of the Hurricane Dennis simulations, cooling in coastal areas is pronounced more than 300 km from the storm center under tropical storm force winds. Vigorous cooling occurs where the existing mixed layer depth is shallow, i.e., within a cyclonic eddy. The rapid reduction of SST due to upwelling here results in a reduced heat energy flux to the atmosphere.

These simulations demonstrate that the heat energy extracted from the ocean away from the storm's central core cannot be neglected. Previous estimates of ocean heat loss to the atmosphere during a tropical cyclone when only considering the heat extracted in the storm core may be too low. The heat utilization may instead vary from 10 to 50% of the initial ocean HHP for a large storm, particularly where the mixed layer is shallow.

**Acknowledgements** This work was sponsored by NOAA, NASA, NSF, and the ONR Secretary of the Navy grant to J. O'Brien. The authors thank Paul Martin, Alan Wallcraft, and the NCOM development team for their assistance with the model. Computations were performed on the IBM SP4 at the Florida State University School of Computational Science.

## References

- Beven J (2005) Hurricane Dennis, 4–13 July 2005. Tropical Cyclone Report, National Hurricane Center
- Bourassa MA (2004) An improved sea state dependency for surface stress derived from in situ and remotely sensed winds. *Adv Space Res* 33:1136–1142
- Bourassa MA, Vincent DG, Wood WL (1999) A flux parameterization including the effects of capillary waves and sea . *J Atmos Sci* 56:1123–1139
- Cione JJ, Uhlhorn EW (2003) Sea surface temperature variability in hurricanes: implications with respect to intensity change. *Mon Weather Rev* 131:1783–1796
- DaSilva A, Young AC, Levitus S (1994) Atlas of surface marine data 1994, vol. 1: algorithms and procedures. NOAA Atlas NESDIS 6, U. S. Department of Commerce
- Ellingsen IH (2004) Internal tides and the spread of river plumes in the Trondheim Fjord. Ph.D. dissertation, Norwegian University of Science and Technology, Trondheim, Norway
- Fox DN, Teague WJ, Barron CN, Carnes MR, Lee CM (2002) The Modular Ocean Data Assimilation System (MODAS). *J Atmos Ocean Technol* 19:240–252
- Holland WR, Chow JC, Bryan FO (1998) Application of a third-order upwind scheme in the NCAR Ocean Model. *J Climate* 11:1487–1493
- Hodur RM, Pullen J, Cummings J, Hong X, Doyle JD, Martin P, Rennick MA (2002) The Coupled Ocean/Atmosphere Meso-scale Prediction System (COAMPS). *Oceanography* 15:88–98
- Kara AB, Barron CN, Martin PJ, Smedstad LF, Rhodes RC (2005) Validation of interannual simulations from the 1/8° global Navy Coastal Ocean Model (NCOM). *Ocean Model* 11:376–398. DOI 10.1016/j.ocemod.2005.01.003
- Large WG, McWilliams JC, Doney S (1994) Oceanic vertical mixing: a review and a model with a nonlocal boundary layer parameterization. *Rev Geophys* 32:63–403
- Leipper DF, Volgenau D (1972) Hurricane heat potential of the Gulf of Mexico. *J Phys Oceanogr* 2:218–224
- Mao Q, Chang SW, Pfeffer RL (2000) Influence of large-scale initial oceanic mixed layer depth on tropical cyclones. *Mon Weather Rev* 128:4058–4070
- Martin PJ (1985) Simulation of the mixed layer at OWS November and Papa with several models. *J Geophys Res* 90:903–916
- Martin PJ (1999) An ocean model applied to the Chesapeake Bay plume. In: Spaulding ML, Butler JL (eds) Estuarine and coastal modeling. Proceedings of the 6th International Conference, pp 1055–1067
- Martin PJ (2000) A description of the Navy Coastal Ocean Model Version 1.0. NRL Report: NRL/FR/7322-009962, Naval Research Laboratory, Stennis Space Center, MS
- Mellor GL, Yamada T (1982) Development of a turbulence closure model for geophysical fluid problems. *Rev Geophys Space Phys* 20:851–875
- Morey SL, Martin PJ, Martin, O'Brien JJ, Wallcraft AA, Zavala-Hidalgo J (2003) Export pathways for river discharged fresh water in the northern Gulf of Mexico. *J Geophys Res* 108: 3303. DOI 10.1029/2002JC001674
- Morey SL, Zavala-Hidalgo J, O'Brien JJ (2005a) The seasonal variability of continental shelf circulation in the northern and western Gulf of Mexico from a high-resolution numerical model. In: Sturges W, Lugo-Fernandez A (eds) Circulation of the Gulf of Mexico: observations and models. Geophysical Monograph Series, pp 203–218. DOI 10.1029/161GM16
- Morey SL, Bourassa MA, Davis XJ, O'Brien JJ, Zavala-Hidalgo J (2005b) Remotely sensed winds for episodic forcing of ocean models. *J Geophys Res* 110:C10024. DOI 10.1029/2004JC002338
- O'Brien JJ (1967a) The non-linear response of a two-layer, baroclinic ocean to a stationary, axially symmetric hurricane: Part 1. Upwelling induced by momentum transfer. *J Atmos Sci* 24:197–207
- O'Brien JJ (1967b) The non-linear response of a two-layer, baroclinic ocean to a stationary, axially symmetric hurricane: Part 2. Upwelling and mixing induced by momentum transfer. *J Atmos Sci* 24:208–215
- Price JF (1981) Upper ocean response to a hurricane. *J Phys Oceanogr* 11:153–173
- Rhodes RC, Hurlburt HE, Wallcraft AJ, Barron CN, Martin PJ, Smedstad OM, Cross S, Metzger JE, Shriver J, Kara A, Ko DS (2002) Navy real-time global modeling systems. *Oceanography* 15:29–43
- Shay LK, Black PG, Mariano AJ, Hawkins JD, Elsberry RL (1992) Upper ocean response to Hurricane Gilbert. *J Geophys Res* 97:20227–20248
- Shen W, Ginis I (2003) Effects of surface heat flux-induced sea surface temperature changes on tropical cyclone intensity. *Geophys Res Lett* 30(18). DOI 10.1029/2003GL017878
- Smith WHF, Sandwell DT (1997) Global seafloor topography from satellite altimetry and ship depth soundings. *Science* 277:1957–1962
- Verschell MA, Bourassa MA, Weissman DE, O'Brien JJ (1999) Model validation of the NASA scatterometer winds. *J Geophys Res* 104:11359–11374

- Walker ND, Leben RR, Balasubramaniam S (2005) Hurricane-forced upwelling and chlorophyll *a* enhancement within cold-core cyclones in the Gulf of Mexico. *Geophys Res Lett* 32. DOI 10.1029/2005GL023716
- Zavala-Hidalgo J, Martinez-Lopez B, Gallegos-Garcia A, Morey SL, O'Brien JJ (2006) Seasonal upwelling on the western and southern shelves of the Gulf of Mexico. *Ocean Dynamics*. DOI 10.1007/s10236-006-0072-3
- Zedler SE, Dickey TD, Doney SC, Price FJ, Yu X, Mellor GL (2002) Analyses and simulations of the upper ocean's response to Hurricane Felix at the bermuda testbed mooring site: 13–23 August 1995. *J Geophys Res* 107(C12). DOI 10.1029/2001JC000969